J Bioenerg Biomembr (2006) 38:83–92
DOI 10.1007/s10863-006-9015-4

ORIGINAL PAPER

Structural and functional analysis of the coupling subunit F in solution and topological arrangement of the stalk domains of the methanogenic A_1A_O ATP synthase

Ingmar Schäfer · Manfred Rössle · Goran Biuković · Volker Müller · Gerhard Grüber

Received: 28 March 2006 / Accepted: 7 April 2006 / Published online: 3 August 2006

Abstract The first low-resolution shape of subunit F of the A_1A_O ATP synthase from the archaeon *Methanosarcina mazei* Gö1 in solution was determined by small angle X-ray scattering. Independent to the concentration used, the protein is monomeric and has an elongated shape, divided in a main globular part with a length of about 4.5 nm, and a hook-like domain of about 3.0 nm in length. The subunit-subunit interaction of subunit F inside the A_1A_O ATP synthase in the presence of 1-ethyl-3-(dimethylaminopropyl)-carbodiimide EDC was studied as a function of nucleotide binding, demonstrating movements of subunits F relative to the nucleotide-binding subunit B. Furthermore, in the intact A_1A_O complex, crosslinking of subunits D-E, A-H and A-B-D was obtained and the peptides, involved, were analyzed by MALDI-TOF mass spectrometry. Based on these data the surface of contact of B-F could be mapped in the high-resolution structure of subunit B of the A_1A_O ATP synthase.

Keywords A_1A_O ATP synthase · A_1 ATPase · *Methanosarcina mazei* Gö1 · Small angle X-ray scattering · F_1F_O ATP synthase · V_1V_O ATPase

Abbreviations BSA: bovine serum albumin · CD: circular dichroism · EDC: 1-ethyl-3-(dimethylaminopropyl) -carbodiimide · IPTG: isopropyl-β-D-thio-galactoside · NTA: nitrilotriacetic acid · PAGE: polyacrylamide gel electrophoresis · PCR: polymerase chain reaction · SAXS: small angle X-ray scattering · SDS: sodium dodecyl sulfate · Tris: Tris-(hydroxymethyl)aminomethane

I. Schäfer · G. Biuković · G. Grüber (✉)
School of Biological Sciences, Nanyang Technological University, 60 Nanyang Drive, Singapore 637551, Singapore
e-mail: ggrueber@ntu.edu.sg

M. Rössle
European Molecular Biology Laboratory, Hamburg Outstation, EMBL c/o DESY, 22603 Hamburg, Germany

V. Müller
Institute of Molecular Biosciences, Molecular Microbiology & Bioenergetics, Johann Wolfgang Goethe-Universität Frankfurt, 60438 Frankfurt, Germany

Introduction

Archaea are a heterogeneous group of microorganisms that often thrive at harsh environmental conditions such as high temperatures, extreme pH's, and high salinity. Like other living cells, they use chemiosmotic mechanisms along with substrate level phosphorylation to conserve energy in form of ATP. Because some archaea are rooted close to the origin in the tree of life, these unusual mechanisms are considered to have developed very early in the history of life and, therefore, may represent first energy conserving mechanisms (Ide et al., 1999; Schäfer et al., 1999). A key component in cellular bioenergetics is the ATP synthase (Pedersen et al., 2000; Senior et al., 2000; Capaldi and Aggeler, 2002). The enzyme from archaea represents a new class of ATPases, the A_1A_O ATP synthases. They catalyze the formation of ATP at the expense of the transmembrane electrochemical ion gradient and are related to the F_1F_O and V_1V_O ATP synthases/ases (Inatomi et al., 1989; Stan-Lotter and Hochstein, 1989; Dirmeier et al., 2000). The A_1A_O ATP synthases are structurally similar to V_1V_O ATPases but synthesize ATP like the F-type ATPases. The membrane-integrated enzyme consists of subunits A–K in the stoichiometry of A_3:B_3:C:D:E:F:H:I:K_x. As its bipartite name implies the A_1A_O ATP synthases is divided into two parts: a water-soluble A_1 ATPase and an integral membrane subcomplex, A_O. ATP is synthesized or hydrolyzed on the A_1 headpiece, consisting of an A_3:B_3 domain, and the energy

provided for or released during that process is transmitted to the membrane-bound A_O domain. The energy coupling between the two active domains occurs via the so-called stalk part (Müller and Grüber, 2003).

The structure of the chemically-driven motor (A_1) from *Methanosarcina mazei* Gö1, which is made up of the five different subunits A_3B_3CDF, was solved by small angle X-ray scattering in solution (Grüber et al., 2001) and image processing of electron micrographs of the negatively stained particles (Coskun et al., 2004a). The data show that the A_1 ATPase is rather elongated, with an A_3:B_3 headpiece and an elongated stalk (Grüber et al., 2001). A comparison of the central stalk of this A_1 complex with bacterial F_1 and eukaryotic V_1 ATPases indicates different lengths of the stalk domain (Grüber et al., 2001). Further insights into the topology of the A_1 ATPase were obtained by differential protease sensitivity (Coskun et al., 2002), and cross-linking studies (Coskun et al., 2002, 2004a). These studies resulted in a model in which the subunits C, D (partly), and F form the central stalk domain (Coskun et al., 2002, 2004a). The first structure of the complete methanogenic A_1A_O ATP synthase was obtained recently by single particle analyses (Coskun et al., 2004b). These studies revealed novel structural features such as a second peripheral stalk, and a collar-like structure. In addition, the membrane-embedded electrically-driven motor A_O is very different in archaea with sometimes novel, exceptional subunit composition and coupling stoichiometries that may reflect the differences in energy conserving mechanisms as well as adaptation to temperatures (Müller and Grüber, 2003).

We have turned our attention to the examination of subunit F of the methanogenic A_1A_O ATP synthase and describe the structural features of this stalk subunit in solution. The location of F and the related stalk subunits D, E and H in the absence and presence of nucleotides have been explored in the intact A_1A_O complex.

Experimental procedures

Materials

ProofStart™ DNA Polymerase and Ni^{2+}-NTA-chromatography resin were received from Qiagen (Hilden, Germany); restriction enzymes were purchased from MBI Fermentas (St. Leon-Rot, Germany). The expression vector pET9d-His_6 was provided by G. Stier, EMBL (Heidelberg, Germany). Chemicals for gel electrophoresis were received from Serva (Heidelberg, Germany). Bovine serum albumin was purchased from GERBU Biochemicals (Heidelberg, Germany). All other chemicals were at least of analytical grade and received from BIOMOL (Hamburg, Germany), Merck (Darmstadt, Germany), Roth (Karlsruhe, Germany), Sigma (Deisenhofen, Germany), or Serva (Heidelberg, Germany).

Constructs and proteins

The gene, encoding subunit F from *M. mazei* Gö1 was amplified using the oligonucleotide primers 5′-CGTTTTCCATGGAGTTAGCAGTGAT-3′ (forward primer) and 5′-TTTGAGCTCTTACTTCCACAGATCAA-3′ (reverse primer), incorporating *Nco*I and *Sac*I restriction sites, respectively (underlined). As template the multicopy vector pTL2 (Lemker et al., 2003) coding for the A_1A_O ATP synthase gene F was obtained from *Escherichia coli* strain DK8 using the standard Nucleobond Plasmid Midi Kit. Following digestion with *Nco*I and *Sac*I, the PCR product was ligated into the pET9d-His_6 vector. The cloned pET9d-His_6 vector containing the DNA fragment, encoding subunit F plus six His-residues at the N-terminus, was transformed into *E. coli* cells (strain BL21) and grown on 30 μg/ml kanamycin-containing Luria-Bertoni (LB) agar-plates. To express His_6-subunit F, liquid cultures were shaken in LB medium containing kanamycin (30 $\mu g\,ml^{-1}$) for about 20 h at 30 °C until an optical density OD_{600} of 0.6–0.7 was reached. To induce production of His_6-subunit F, the cultures were supplemented with isopropyl-β-D-thio-galactoside (IPTG) to a final concentration of 1 mM. Following incubation for another 4 h at 30 °C, the cells were harvested at 10 000 × *g* for 20 min, 4 °C. Subsequently, they were lysed on ice by sonication for 3 × 1 min in buffer A (50 mM Tris/HCl, pH 8.5, 100 mM NaCl, 4 mM Pefabloc SC (BIOMOL). The lysate was cleared by centrifugation at 10 000 × *g* for 30 min at 4 °C, the supernatant was passed through a filter (0.45 μm pore-size) and supplemented with Ni^{2+}-NTA resin. The His-tagged protein was allowed to bind to the matrix for 90 min at 4 °C and eluted with an imidazole-gradient (25–200 mM) in buffer A by mixing on a sample rotator (Neolab). Fractions containing His_6-subunit F were identified by SDS-PAGE[1] (Laemmli, 1970), pooled, concentrated using Centriprep YM-10 (3 kDa molecular mass (MM) cut off) spin concentrators (Millipore), and subsequently applied on an ion-exchange column (Resource Q (6 ml), Amersham Biosciences), equilibrated in a buffer of 50 mM Tris/HCl (pH 8.5) and 100 mM NaCl. The purity of the protein sample was analyzed by SDS-PAGE (Laemmli, 1970). The SDS-gels were stained with Coomassie Brilliant Blue G250. Protein concentrations were determined by the bicinchonic acid assay (BCA; Pierce, Rockford, IL. USA).

The methanogenic A_1A_O ATP synthase of *Methanococcus jannaschii* was purified by sucrose density centrifugation and anion exchange chromatography (DEAE-Sepharose) as described previously (Lingl et al., 2003). ATPase active fractions were pooled and concentrated on Centricon

100 kDa concentrators (Millipore). The concentrated sample was loaded on a Superose 6 column (10/30, Amersham Biosciences) and eluted with 50 mM Tris/HCl (pH 7.5), 5 mM $MgCl_2$, 10% glycerol, 150 mM NaCl, 0.1% Triton X-100, 0.1 mM PMSF and 1 mM Pefabloc SC (BIOMOL) (Coskun et al., 2004b).

Determination of native molecular mass

Gel filtration chromatography was performed using a Superdex 75 HR 10/30 column (Amersham Biotech) using a buffer of 50 mM Tris/HCl (pH 8.5) and 100 mM NaCl. To construct a calibration curve, a set of standard proteins (Amersham Biotech and Sigma) was analyzed. The K_{av} parameter was determined ($K_{av} = (V_e - V_0)/(V_t - V_0)$, where V_e represents the elution volume, V_0 the void volume, and V_t the total bed volume). The K_{av} values for standard proteins were plotted as a function of the logarithm of molecular mass, and the resulting calibration curve was used to derive the MM of subunit F.

CD spectroscopy

Steady state CD spectra were measured in the far UV-light (185–255 nm) using a CHIRASCAN spectropolarimeter (Applied Photophysics). Spectra were collected in a 50 μl quartz cell (Hellma) at 18 °C at a step resolution of 0.1 nm. CD spectroscopy of subunit F (1.0 mg/ml) was performed in 50 mM Tris/HCl, pH 8.5, and 100 mM NaCl and 1 mM DTT. Ten scans were averaged to obtain a final spectrum. The spectrum for the buffer was subtracted from the spectrum of subunit F. This baseline corrected spectrum was used as input for computer methods to obtain predictions of secondary structure. In order to analyze the CD spectrum the analysis programmes CONTIN (Provencher, 1982) and SELCON (Screerama and Woody, 1993) were used.

X-ray scattering experiments and data analysis of subunit F

The synchrotron radiation X-ray scattering data were collected following standard procedures on the X33 camera (Boulin et al., 1986, 1988) of the EMBL on the storage ring DORIS III of the Deutsches Elektronen Synchrotron (DESY). The scattering patterns from subunit F at protein concentrations of 4.9, 9.7 and 19.5 mg/ml were measured by means of an image plate detector (MAR345; Marresearch, Norderstedt, Germany) setup with the sample—detector distances of 2.4 m, covering the range of momentum transfer $0.1 < s < 4.5\,\mathrm{nm}^{-1}$ ($s = 4\pi\sin(\theta)/\lambda$, where θ is the scattering angle and $\lambda = 0.15$ nm is the X-ray wavelength). The data were normalized to the intensity of the transmitted beam and the scattering of the buffer was subtracted as background. These difference curves were scaled for concentration which allows evaluation of the molecular mass (MM) by the forward scattering $I(0)$ and the radius of gyration R_g using the Guinier (Guinier, 1939) approximation. All the data processing steps were performed with the program package PRIMUS (Konarev et al., 2003). The distance distribution function $p(r)$ of the particle was computed by the indirect transform package GNOM (Svergun et al., 1993). For the MM estimation the forward scattering of a bovine serum albumin (BSA) solution was taken as reference.

Two low resolution models of the F subunit were built by the program DAMMIN (Svergun, 1992) and GASBOR (Svergun, 1997) as described in (Armbrüster et al., 2004). Both approaches start with an ensemble of densely packed dummy atoms (DAMMIN) or dummy residues (GASBOR) inside a search volume defined by a sphere of diameter D_{max}. Ten independent GASBOR reconstructions were computed and the models were further analyzed using the packages DAMAVER (Svergun et al., 2001) and SUBCOMP resulting in an averaged model for the shape representation. The scattering intensity of the ε-subunit from the F_1F_O ATPsynthase was computed based on the 1AQT pdb entry using the program CRYSOL (Svergun and Koch, 2002).

Cross-link formation in the A_1A_O ATP synthase

After preincubation of the A_1A_O ATP synthase from *Methanococcus jannaschii* with 5 mM nucleotide and $MgCl_2$, respectively, for 5 min, cross-linking was induced by supplementation with 5 mM of 1-ethyl-3-(dimethylaminopropyl)-carbodiimide (EDC) as a crosslinker for 30 min on a sample rotator at room temperature. The reaction was stopped by addition of Laemmli buffer (63 mM Tris/HCl, pH 6, 10% glycerin, 2% SDS and 0.01% Bromphenolblue). Samples were dissolved in DTT-free dissociation buffer, and applied to an SDS-polyacrylamide gel as described above. The subunits involved in cross-linking were identified by MALDI-TOF analysis.

Tryptic digest and MALDI-TOF analysis

The crosslinked products of the A_1A_O ATP synthase were cut from the gel and destained overnight with a solution of 50 mM ammonium bicarbonate, 40% ethanol. The protein was digested in gel with trypsin (Promega) according to Roos et al. (1998) except that the bands had been washed three times with acetonitrile before drying them in a speed vacuum concentrator. Digested samples were desalted with a C18ZipTip (Millipore) and eluted with CHCA—(10 mg/ml α-cyano-4-hydroxycinnamic acid in 50% acetonitrile, 0.1% trifluoroacetic acid) or FA—(8 mg/ml 3-methoxy-4-hydroxycinnamic acid in 50% acetonitrile, 0.1% trifluoroacetic acid) matrix solution.

1–2 μl of matrix-analyte solution was spotted onto the MALDI plate and allowed to dry. Peptide mass mapping was performed by matrix assisted laser desorption-ionisation/time-of-flight mass spectrometry (MALDI-TOF MS) using a Bruker Reflex III^{TM} MALDI-TOF spectrometer (Bremen, Germany). The peptide map was acquired in reflectron positive-ion mode with delayed extraction at a mass range of 100–5 000 Da. The instrument was calibrated using a calibration mixture (Applied Biosystems). For interpretation of the protein fragments, the PEPTIDEMASS (Wilkins et al., 1997) program available at Expasy web site (www.expasy.ch/tools/peptide-mass.html) was used.

Results

Purification of subunit F from *M. mazei* Gö1

Induction of His-tagged protein synthesis under the conditions specified in "EXPERIMENTAL PROCEDURES" resulted in an approximately 14 kDa protein which was found entirely within the soluble fraction. A Ni^{2+}-NTA resin column and an imidazole-gradient (25–200 μM) in buffer consisting of 50 mM Tris/HCl (pH 8.5) and 100 mM NaCl was used to separate His_6-subunit F from the main contaminating proteins. Subunit F eluting at 100 mM imidazol was collected and subsequently applied to a RESOURCE^{TM} Q column. Analysis of the isolated protein by MALDI mass spectrometry revealed the high purity of the subunit, and that the protein had the sequence-based predicted mass of 12,217 Da.

CD spectroscopy of subunit F

The CD spectrum of subunit F was measured between 185–255 nm (Fig. 1). The minima at 220 and 208 nm and the maximum at 192 nm indicate the presence of α-helical structures in the protein; the overall spectrum is characteristic for a protein with mixed α/β structure. Several computer based methods were used to analyze the CD spectrum of subunit F. The secondary structure content calculated was 43% α-helix and 33% β-sheet.

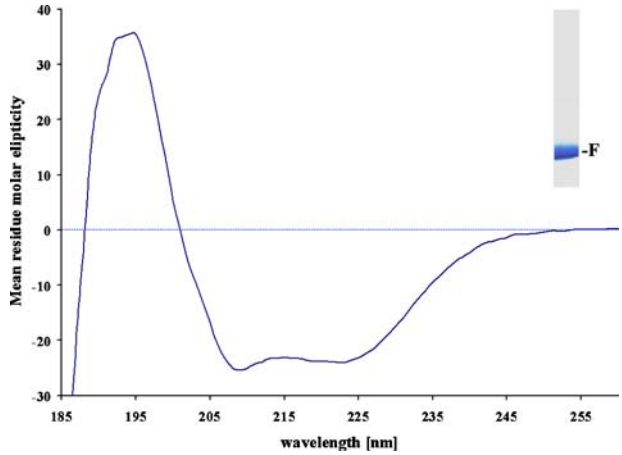

Fig. 1 Far UV-CD spectrum of subunit F from *M. mazei* Gö1. (Insert), SDS-gel shows a sample of the His_6-subunit F used in the CD spectroscopy measurement

Determination of molecular mass and overall dimensions of the native F subunit

In order to determine the native molecular mass of subunit F from *M. mazei* Gö1, a Superdex 75 gel filtration column was calibrated by determining the K_{av} values for a set of standard proteins of known MM (Fig. 2A). A calibration curve based on these K_{av} values is shown in Fig. 2B. Comparison of the K_{av} for subunit F *versus* the standard proteins suggests the native molecular mass (MM) of approximately 15 $\pm$ 2 kDa. In a complementary approach, SAXS patterns from solutions of subunit F were recorded and processed as described in "EXPERIMENTAL PROCEDURES" to yield

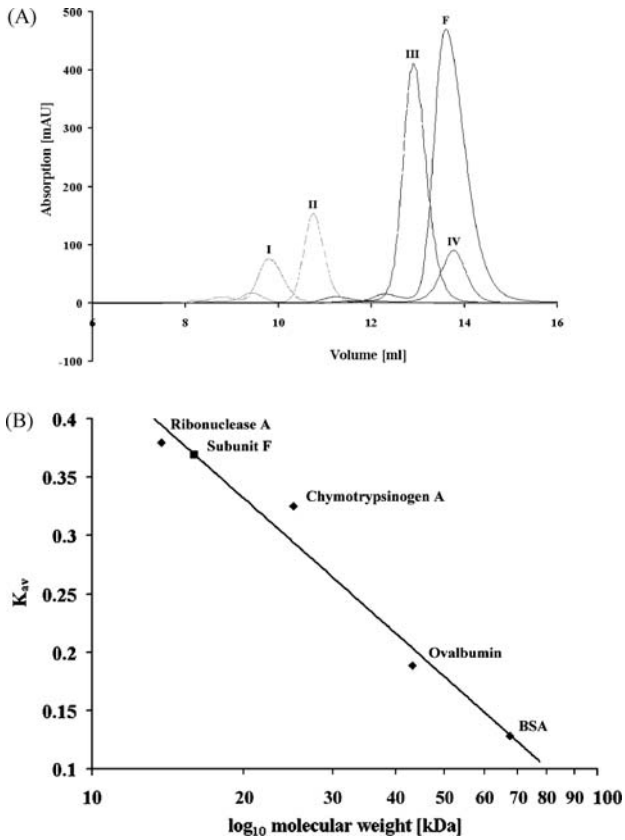

Fig. 2 Determination of the native molecular mass by gel filtration analysis. (A) Superdex 75 gel filtration analysis of subunit F was performed as described under "EXPERIMENTAL PROCEDURES". Proteins used as molecular size standards (◆) were BSA ((I) 67 kDa), ovalbumin ((II) 45 kDa), β-chymotrypsin A ((III) 25 kDa) and ribonuclease A ((IV) 13.7 kDa). (B), for each protein, a K_{av} parameter was derived as described under "EXPERIMENTAL PROCEDURES". The K_{av} for subunit F is indicated by (■)

the final composite scattering curve in Fig. 3A. The radius of gyration R_g and the maximum dimension D_{max} of subunit F are 2.03 ± 0.02 nm and 7.5 ± 0.2 nm, respectively, suggesting that the subunit is a rather elongated particle. Comparison with the scattering from the reference solutions of BSA yields the estimate of MM of 14 ± 4 kDa, in agreement with the results of the gel filtration chromatography and indicating that subunit F is monomeric at the concentrations used. However, the determined MM of the native molecule is somewhat larger than expected from analysis of the dehydrated protein in the MALDI-TOF experiment (12,217 Da) and the amino acid sequence (11,890 Da; Expert Protein Analysis System (Wilkins et al., 1997)). This may be attributed to a high hydration of the particle in solution, characteristic for extended molecules with a large specific surface accessible to the solvent. The excluded (Porod) volume of the hydrated particle in solution was $180 \pm 5\,nm^3$ (compared to the dry particle volume of $54\,nm^3$ computed from the sequence) also suggesting a rather high hydration of subunit F. The distance distribution function $p(r)$ (Fig. 3B) further confirms that subunit F is an elongated particle with the average radius of cross-section of about 3 nm as reflected by the main maximum of the $p(r)$ function. The shoulder at larger intraparticle distances indicates that the particle consists of two distinct domains with the average distance between their centers of about 4 nm.

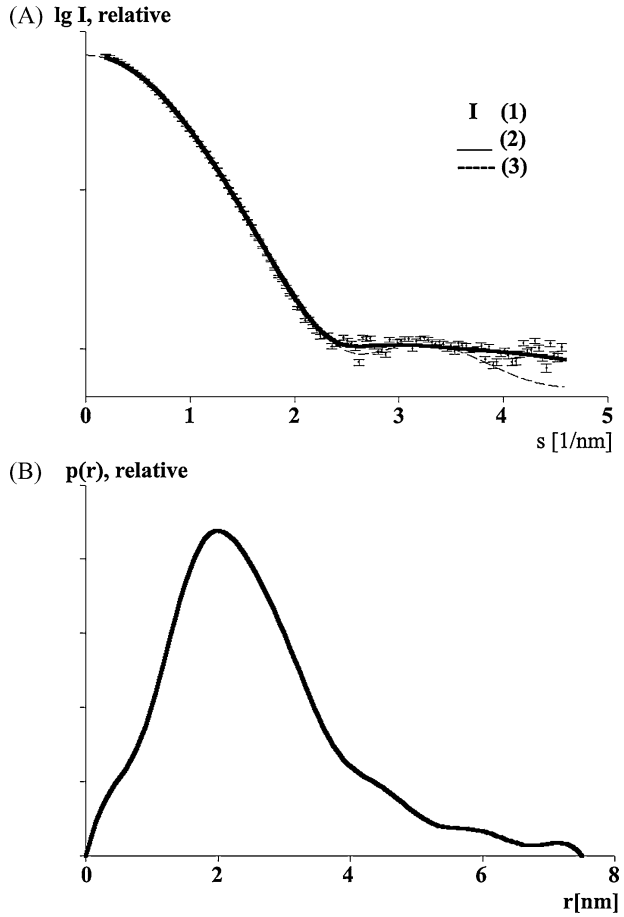

Fig. 3 X-ray scattering patterns from subunit F of *M. mazei* Gö1. (A) experimental SAXS curve from subunit F (1), scattering from typical *ab initio* model of subunit F (2) computed by the program GASBOR (18) and (3) scattering pattern from the high resolution model of subunit ε ((32) PDB code 1AQT) calculated by the program CRYSOL. (B) The distance distribution function of subunit F was computed from the experimental data by the program GNOM

Shape and domain structure of subunit F from *M. mazei* Gö1

The gross structure of subunit F was restored *ab initio* from the scattering pattern in Fig. 3A using the shape determination program DAMMIN and the dummy residues modeling program GASBOR as described in "EXPERIMENTAL PROCEDURES". The two approaches yielded similar results but the models provided by DAMMIN could only fit the data up to $s = 0.25\,nm^{-1}$ and therefore resulted in lower resolution. In the following, the models obtained with GASBOR are presented, which yield good fits to the experimental data in the entire scattering range (a typical fit displayed in Fig. 3, curve 2, has the discrepancy $\chi = 1.39$). Ten independent reconstructions yielded reproducible models and the average model and the most probable model are displayed in Fig. 4. Subunit F appears as an elongated molecule with two distinct domains, a main globular with a length of about 4.5 nm, and a hook-like domain of about 3.0 nm in length. This gross structure resembles very much the shape of the homolog ε subunit of the related F_1F_O ATP synthase from *Escherichia coli* (Fig. 4) available in the PDB (Bernstein et al., 1977) (entry 1AQT). Moreover, the scattering pattern computed from the model of subunit ε displays a fair agreement to the scattering by subunit F in the entire range of scattering angles (Fig. 3, curve 3, $\chi = 2.5$). Deviations observed at the very small angles point to a somewhat more extended appearance (or, possibly, a higher hydration) of subunit F from *M. mazei* Gö1 compared to subunit ε, but the overall resemblance is still remarkable. The known atomic model of ε was positioned inside the low resolution model of subunit F (Fig. 5). The N-terminal barrel of ε is well accommodated within the global domain of subunit F and the anti-parallel two α-helix hairpin of the C-terminus of subunit ε fits the hook-like shape of subunit F (Fig. 5A). An elongated shape has also been described most recently for subunit F of the related prokaryotic V-ATPase from *Thermus thermophilus* ((*Tt*-F), Figs. 4 and 6 (Makyio et al., 2005)). The atomic model of this subunit is well accommodated within the shape of subunit F from *M. mazei* Gö1 (Fig. 6A, B). The N-terminal and C-terminal part of the *Tt*-F subunit lies in the main globular and the hook-like domain of subunit F of *M. mazei* Gö1, respectively.

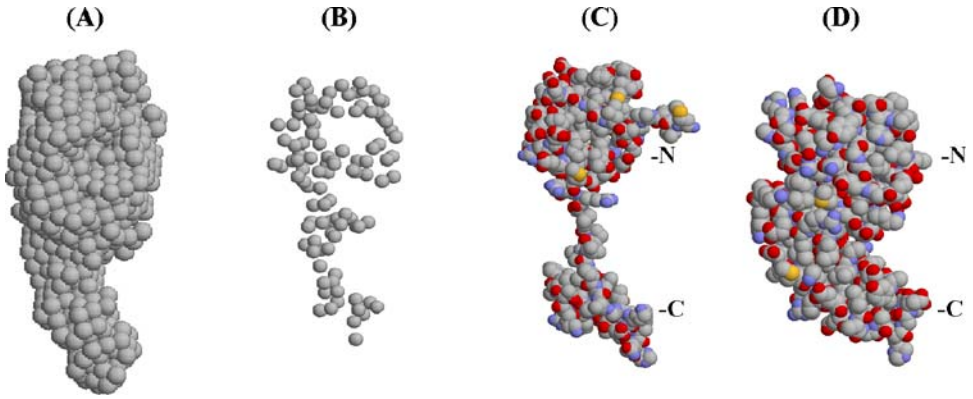

Fig. 4 Models of the subunits F_{Mm}, ε and F_{Tt}. Column (A) and (B), averaged and most probable models of subunit F from *M. mazei* Gö1 displayed as beads and dummy residues, respectively. (C) and (D), high resolution model of subunit F and ε of the related prokaryotic V_1V_O ATPase from *T. thermophilus* (32) and the F_1F_O ATPsynthase from *E. coli* ((39) PDB code 1AQT), respectively; the N- and C-termini are indicated

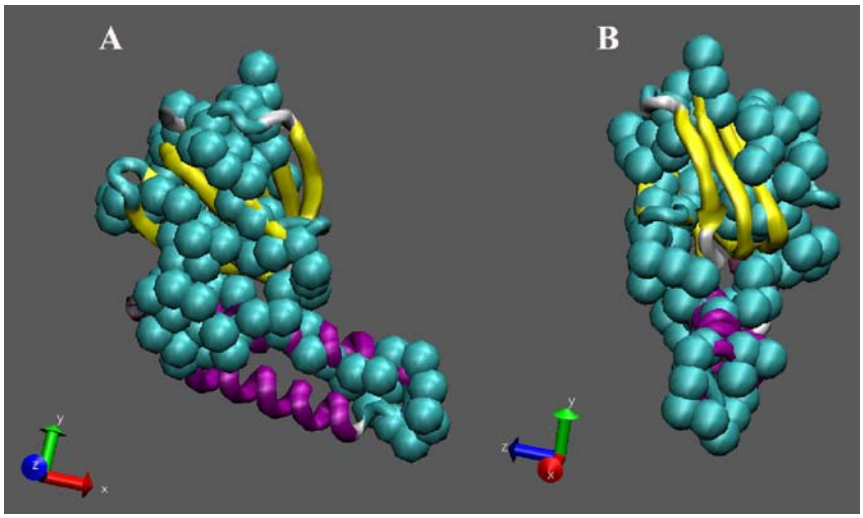

Fig. 5 Superposition of the GASBOR model with the ε-subunit from the F_1F_O ATPsynthase. The side—(A) and front view (B) indicate a similar composition of the F subunit from *M. mazei* Gö1 (green atoms) in respect with the ε-subunit. As for the subunit ε a two domain composition of the F-subunit from *M. mazei* Gö1 can be proposed. The N-terminal barrel of ε and the anti-parallel two α-helix hairpin of the C-terminus of subunit ε is shown in yellow and lilac, respectively

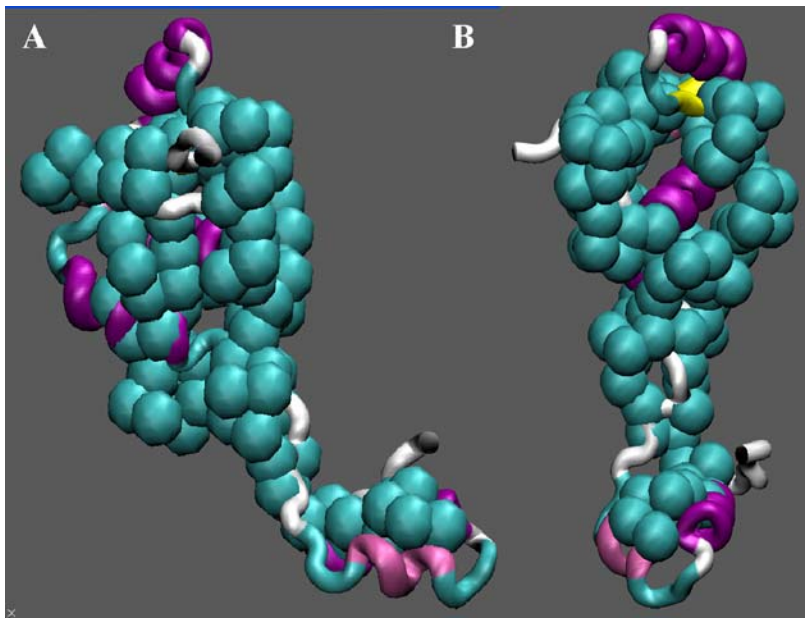

Fig. 6 Superposition of the GASBOR model of F_{Mm} with subunit F_{Tt} from *T. thermophilus*. Comparison of the side—(A) and front view (B) of the F subunit from *M. mazei* Gö1 (green atoms) and subunit F_{Tt} from *T. thermophilus*. The N-terminal barrel of F_{Tt} and the anti-parallel two α-helix hairpin of the C-terminus of this subunit is shown in yellow and lilac, respectively

Cross-linking of A_1A_O ATP synthase subunits induced by EDC

Recently, we have shown, that subunit B and F does form a crosslink product in the A_3B_3CDF complex from *M. mazei* Gö1 (Coskun et al., 2004a). In order to investigate whether this formation does also occur in the whole complex in the presence of different nucleotides, and whether this close proximity of both subunits is also common to other sources, the intersubunit crosslinking of both polypeptides inside the A_1A_O ATP synthase from *Methanococcus jannaschii* was studied, using the cross-linking reagent EDC, which results in cross-linking of carboxyl and amino groups. Fig. 7 illustrates the results of crosslinking of the A_1A_O ATP synthase with EDC under different nucleotide conditions. When the enzyme was incubated with 5 mM MgAMP-PNP at 4 °C before EDC-treatment, a 63 kDa product (II), composed of the subunits B (51 kDa) and F (12 kDa) could be identified by MALDI mass spectrometry. The B-F product is formed by the peptides $_{388}$DLVAVVGEEALTDR$_{401}$ and $_{82}$IDPVKELIR$_{90}$ of the subunits B and F, respectively. By comparison, the presence of MgATP leads to lower crosslink formation, which disappeared, when the A_1A_O complex was incubated in the presence of MgADP+P_i and MgADP.

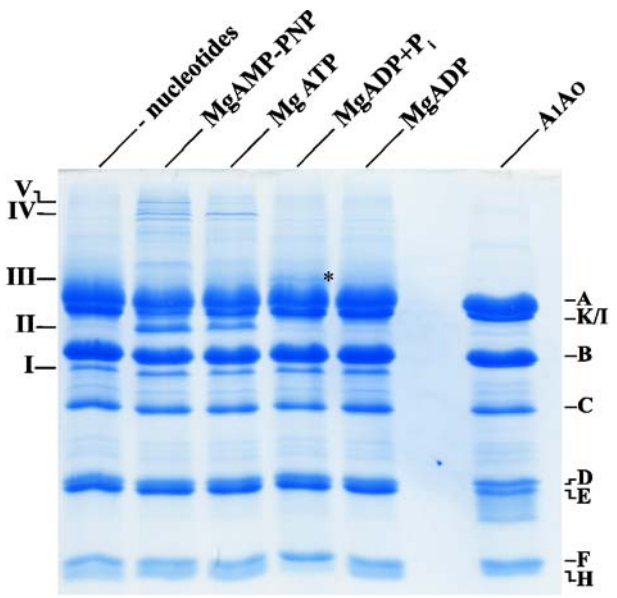

Fig. 7 Cross-linking of the methanogenic A_1A_O ATP synthase from *M. jannaschii* using EDC. A_1A_O ATP synthase was incubated with 5 mM MgAMP-PNP (*lane 2*), MgATP, MgADP + P_i, MgADP or without nucleotide (*lane 1*) for 5 min at 7 °C, followed by addition of 5 mM EDC for 30 min at room temperature and stopped by addition of Laemmli buffer containing 63 mM Tris/HCl, pH 6, 10% glycerol, 2% SDS and 0.01% Bromphenolblue. The samples were applied to a 15% total acrylamide and 0.4% crosslinked acrylamide gel. Lane 6, A_1A_O ATP synthase in the presence of 50 μm of dithiothreitol (DTT). The crosslink products are labeled I-V and the (*) represent the crosslink formation III (A-H)

Furthermore, when the enzyme was supplemented with EDC in the presence of MgAMP-PNP six new bands were generated. Besides the mentioned B-F formation (II), the products I, IV and V could be unequivocal identified by MALDI mass spectrometry, demonstrating that band I (48 kDa) derived from subunit D (25 kDa) and E (23 kDa) (Table 1). The bands IV and V include the subunits A-B-D and A-B oligomer-formation. When the enzyme was suspended in MgATP, the cross-link products I, II and IV were obtained, with a slight decrease of the B-F (II) formation (s. above). In the presence of MgADP + P_i the B-F (II), A-B-D (IV) and A-B oligomer formations (V) disappeared and a new band (III) with an apparent molecular mass of about 78 kDa was obtained. This product was formed by the subunits A and H, which goes along with the disappearence of the H subunit. The crosslink occurred via the peptides $_{106}$TGSIFIPRGVDVPALPR$_{122}$ and $_{74}$ILEETEK$_{80}$ of subunit A and H, respectively.

Discussion

Knowledge of the structure of proteins in conditions close to physiological is essential for understanding their functional roles. X-ray scattering in solution allows the determination of the overall structure of native biological macromolecules and was successfully applied for the solution structure of the chitin binding protein (Svergun et al., 2000), the F_1 ATPase (Svergun et al., 1998), the V_1 ATPase (Svergun et al., 1998) or subunit C of the V-ATPase (Armbrüster et al., 2004), whose structural features were confirmed by X-ray crystallography (Gibbons et al., 2000; Radermacher et al., 2001; Vaaje-Kolstad et al., 2005) and/or 3D reconstructions from electron micrographs (Drory et al., 2004). Also determined from solution X-ray scattering data was the hydrated A_3B_3CDF complex from the methanogenic A_1A_O ATP synthase (Grüber et al., 2001), showing that the central stalk is rather elongated with 8.4 nm in length. Together with the 3D reconstruction of this complex (Coskun et al., 2004a), derived from negatively stained particles, the subunits D, F and C could be located inside the central stalk domain, whereby the nucleotide-binding subunits A and B form the hexameric headpiece, in which part of subunit D penetrates. The present low-resolution structure of the hydrated F subunit with a length of 7.5 nm would partially span the width of the central stalk. As indicated by the initial portion of the scattering intensity, the protein is monodisperse and homogeneous in solution, independent of the concentration used (4.5–19.5 mg/ml). The fact that subunit F (F_{Mm}) of the *M. mazei* Gö1 A_1A_O ATP synthase is exclusively elongated in solution is supported by the apparent size based on exclusion chromatography. Its shape is remarkably similar in the overall structure to that of the proposed homolog ε of the *Escherichia coli* F_1F_O ATP synthase (Uhlin et al., 1997) and

Table 1 MALDI-mass spectrometry analysis of peptides involved in the cross-linking product D-E (I), B-F (II) and A-H (III), respectively

Subunit	Start residue	End residue	Measured mass	Sequence
D	4	8	726.5	VNPTR
	14	23	1596.8	LKNKIKLAEK
	127	134	986.2	LDEAAKK[a]
	166	178	1971.2	VNALEYVIIPRLK
	188	200	2191.0	LDEMERENFFRLK
E	16	22	1029.3	AEVSRIK
	42	50	1212.0	KTLGDSLAK
	72	79	1291.8	RITLNKRK
	119	130	1766.5	AYSSKESEELVK[a]
B	14	45	3939.1	SIAGPLLIVEGVEGAAYGEIVEVICPDGEKR
	72	83	1978.4	DTRVRFTGRTAK
	127	148	3137.3	KVPSDFIQTGISTIDGMNTLVR
	300	336	5273.2	TGTITQIPILTMPDDDITHPIPDLTGYITEGQIVLSR
	366	371	954.3	TREDHK
	388	401	1777.0	DLVAVVGEEALTDR[b]
	427	448	3317.6	SIEETLDLLWELLAILPEEELK
F	17	27	1425.2	LAGLTDVYEVK
	68	75	1152.8	VIVEIPDKHGK
	76	86	1582.9	HGKLERIDPVK
	82	90	1866.9	IDPVKELIR[b]
A	14	28	1726.2	IIKIAGPVVVAEGMK
	106	122	2338.8	TGSIFIPRGVDVPALPR[c]
	313	324	2109.2	EASVYTGITIAEYFR
	420	432	2039.5	VFWALDANLAR
	544	553	1348.5	AVERGVEPAK
H	11	21	1672.4	EVKLAEEQAVK
	35	43	1444.2	AEAIEEAKK
	42	53	1686.3	KLIAEAEEEAK
	61	68	1073.2	KAEEEAK
	74	80	824.4	ILEETEK[c]

[a]Peptides involved in the crosslink product I (D-E).

[b]Peptides involved in the crosslink product II (B-F).

[c]Peptides involved in the crosslink product III (A-H).

subunit F (F_{Tt}) of the related prokaryotic V-ATPase from *Thermus thermophilus* (Makyio et al., 2005), composed of a globular part, made up by the N-terminal region (Figs. 5 and 6) and a hook-like part, which is formed by the C-terminus, respectively. This indicates that the three subunits not only display the same overall appearance but also have similar domain structure, although subunit F_{Mm} shows a sequence identity of 9% and 17% to subunit ε and F_{Tt}, respectively. The same phenomenon has been described recently for subunit C and H of the eukaryotic V-ATPase with a sequence identity of only 14%, but a similar overall shape, making both subunits to structural and functional components which bridge the V_1 and V_O part (Armbrüster et al., 2004).

As shown in the A_3B_3DF complex and the A_1A_O ATP synthase from *M. mazei* Gö1 (Coskun et al., 2004a) and *M. jannaschii* (Fig. 7), subunit F can be cross-linked to the nucleotide-binding subunit B, independent of whether dithiobis [sulfosuccinimidylpropionate] (DSP with a length of 1.2 nm) (Coskun et al., 2004a) or the zero-length 1-ethyl-3-(dimethylaminopropyl)-carbodiimide (EDC) was used. The zero-length crosslink is formed between the C-terminal region $_{388}$DLVAVVGEEALTDR$_{401}$ and $_{82}$IDPVKELIR$_{90}$ of subunit B and F, respectively. The recent high resolution structure of the non-catalytic B subunit of the methanogenic A_1A_O ATP synthase (Schäfer et al., 2006) shows that the $_{388}$DLVAVVGEEALTDR$_{401}$ peptide is at a similar position to the so-called DELSEED-region of the nucleotide-binding subunits α and β of the F_1F_O ATP synthases, which form a disulphide bond with the C-terminal helix of the coupling subunit ε (Aggeler et al., 1995). Crosslinking by EDC also showed that subunit F_{Mm} is in close contact to the stalk subunits C and D (Coskun et al., 2004a). By comparison, the N-terminal domain of subunit ε and F_{Tt} is in close contact to the rotary subunit (Makyio et al., 2005) and D (Wilkens et al., 1995) of the F-ATP synthase and the prokaryotic V-ATPase, respectively. Taken together, the data demonstrate that subunit F of the methanogenic ATP synthase not only shares a similar overall architecture with an N-terminal- and a C-terminal hook-like part but also arrangements inside the enzyme with homolog subunits. Therefore, we suggest that the globular part of subunit F_{Mm} emerges from the bottom domain of the central stalk of A_1, where it interacts with both subunits C and D, and goes up until the C-terminal hook-like domain of F_{Mm} reaches its crosslink partner subunit B in

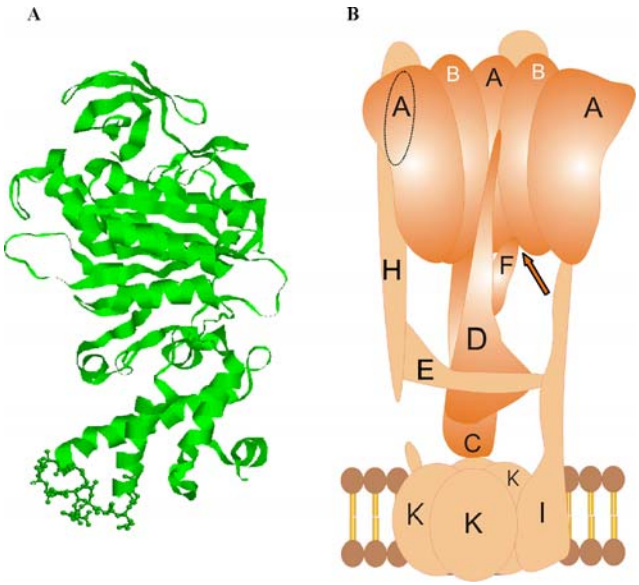

Fig. 8 Structural model of the non-catalytic B subunit (A) and the subunit arrangement in the methanogenic A_1A_O ATP synthase (B). (A) The atomic model of subunit B from the *M. mazei* Gö1 A_1A_O ATP synthase derived from the X-ray coordinates determined recently (Schäfer et al. (2006); PDB 2c61). The C-terminal region interacting with subunit F (F_{Mm}) is labeled by sticks and balls and by an arrow in the topological model (B). (B) A_1- and A_O subunits are labeled in orange and beige, respectively. The subunit topology in the A-type ATP synthase is based on biochemical (11, 12, this work) and structural data (10, 13, this work). The ellipse indicates the crosslink region of subunit A and H, which occurs from the backside of the catalytic A subunit (see text)

the A_1 headpiece (Fig. 8A). In addition, a crosslink product of subunit ε with the non-catalytic α subunit was obtained preferentially in the MgATP-state of the F_1F_O ATP synthase (Aggeler and Capaldi, 1996). By comparison, nucleotide-dependent cross-linking of the A_1A_O ATP synthase from *M. jannaschii* with EDC shows that B-F formation is high in the presence of the non-hydrolyzable ATP-analogue, MgAMP-PNP (Fig. 7). Such subunit-subunit interaction is absent when the enzyme is suspended in MgADP + Pi or MgADP, implying that subunit F movement is dependent on the nucleotide bound to the A_1A_O ATP synthase. This observation supports the recently decribed nucleotide-dependent crosslinking of B-F in the A_1 ATPase from *M. mazei* Gö1 with DSP (Coskun et al., 2004a), indicating that this rearrangement of both subunits can be generalized for A_1A_O ATP synthases. The structural and biochemical data reported suggest the coupling function of subunit F in the methanogenic A_1A_O ATP synthase. The protein exceeds the distance between the nucleotide-binding subunit B and the bottom of the central stalk and provides the physical and structural linkage between the nucleotide-binding events in the A_3B_3 headpiece of A_1 with the ion-coupling in the A_O portion.

Our data also show a nucleotide dependent movement of subunit H, which becomes crosslinked via its C-termius ($_{74}$ILEETEK$_{80}$) with the N-terminal domain of subunit A ($_{106}$ TGSIFIPRGVDVPALPR$_{124}$) in the presence of MgADP + P_i. This N-terminal peptide of subunit A belongs to the so-called "non-homologous region" in the A subunits, an insert of an 80–90 amino acids long loop, which is similar to the catalytic A subunits in A-ATP synthase but also the related V-ATPases (Gasteiger et al., 2003). The atomic model of subunit A of the A_1A_O ATP synthase from *Pyrococcus horikoshii* ((Olendzenski et al., 1998) pdb 1vdz) yields this insert as a protuberance in the upper part of subunit A, which enables subunit H to bind and form a peripheral stalk subunit as shown in Fig. 8. Previously, we have shown by 2D projections from electron micrographs of the methanogenic A_1A_O ATP synthase that the A_3B_3 headpiece is connected via two peripheral stalk (Coskun et al., 2004). One of these stalks appears to be in close contact with two areas of the A_1 headpiece, with one located at the outside and the second on top of the A_3B_3 headpiece (Fig. 8B). This peripheral stalk shows a clear connection to the A_O portion via the collar structure and is predicted to be formed by subunit I (Coskun et al., 2004). The second peripheral stalk appears to be connected to the collar domain and goes up to the A_1 headpiece. Likely candidates for this stalk are the remaining A_1A_O hydrophilic subunits H (12 kDa) and E (25 kDa) (Coskun et al., 2004). The modest contact area of this peripheral stalk with the A_1 headpiece, which is also evident in electron micrographs of the related bacterial V_1V_O ATPase from *Caloramator fervidus* (Boekema et al., 1999), was discussed to be caused partially by stain accumulation. Here we not only demonstrate that it is subunit H which is in direct contact with subunit A, but also that this interaction depends on nucleotide-binding to the catalytic site. Whether this rearrangement might be involved in coupling processes has to be analyzed in future studies. The crosslink experiments show also light on the topology of the subunits D and E with respect to each other. Subunit D and E can be crosslinked readily via the peptides $_{127}$LDEAAKK$_{134}$ and $_{119}$AYSSKESEELVK$_{130}$, respectively, independent of the nucleotide added. This supports the view that subunit H forms the upper part of the second peripheral stalk, whereby subunit E is in close contact to the central stalk subunit D, and thereby forms at least partially the collar domain.

In summary, the data presented demonstrate that subunit F of the *M. mazei* Gö1 ATP synthase exists in solution as an elongated molecule, organized as two well-defined domains, as determined by two *ab initio* shape restoration procedures. The similarity in shape, domain structure and nucleotide dependent arrangements of both subunit F and the related ε subunit of the bacterial F_1F_O ATP synthase is in line with their function in coupling the catalytic events in the A_1/F_1 and A_O/F_O portions. Furthermore, the EDC induced crosslinking data of the intact A_1A_O ATP synthase provide the structural basis towards a more complete understanding of the central and peripheral stalks inside the enzyme. Whether the

nucleotide-dependent rearrangement of the peripheral stalk subunit H might act as a coupling or regulatory domain in the A_1A_O ATP synthase, as described for peripheral stalk of the plant V_1V_O ATPase (Domgall et al., 2002), can now be addressed.

Acknowledgments We thank Dr. A. Grüber for mass spectrometry measurements and Mrs. A. Armbrüster for technical assistance. We acknowledge the support of Dr. S. Bailer in approaches of molecular biology. We thank Prof. S. Iwata (Imperial College, London) making the structural data of subunit F from *T. thermophilus* available. This research was supported by the School of Biological Sciences, Nanyang Technological University, Singapore.

Bibliography

Aggeler R, Haughton MA, Capaldi RA (1995) J Biol Chem 270:9185–9191
Aggeler R, Capaldi RA (1996) J Biol Chem 271:13888–13891
Armbrüster A, Svergun DI, Coskun Ü, Juliano S, Bailer SM, Grüber G (2004) FEBS Lett 570:119–125
Bernstein FC, Koetzle TF, Williams GJB, Meyer EG, Jr, Brice MD, Rodgers JR, Kennard O, Shimanouchi T, Tasumi M (1977) J Mol Biol 112:535–542
Boekema EJ, van Bremen, JFL, Brisson A, Ubbink-Kok T, Konings WN, Lolkema JS (1999) Nature 401:37–38
Boulin C, Kempf R, Koch MHJ, McLaughlin SM (1986) Nucl Instrum Meth A 249:399–407
Boulin CJ, Kempf R, Gabriel A, Koch MHJ (1988) Nucl Instrum Meth A 269:312–320
Capaldi RA, Aggeler R (2002) TIBS 27:154–160
Coskun Ü, Grüber G, Koch MHJ, Godovac-Zimmermann J, Lemker T, Müller V (2002) J Biol Chem 277:17327–17333
Coskun Ü, Radermacher M, Müller V, Ruiz T, Grüber G (2004a) J Biol Chem 279:22759–22764
Coskun Ü, Chaban YL, Lingl A, Müller V, Keegstra W, Boekema EJ, Grüber G (2004b) J Biol Chem 279:38644–38648
Dirmeier R, Haska G, Stetter KO (2000) FEBS Lett 467:101–104
Domgall I, Venzke D, Luttge U, Ratajczak R, Böttcher B (2002) J Biol Chem 277:131115–13121
Drory O, Frolow F, Nelson N (2004) EMBO Rep 5:1148–1152
Gasteiger E, Gattiker A, Hoogland C, Ivanyi I, Appel R D, Bairoch A (2003) Nucleic Acids Res 31:3784–3788
Grüber G, Svergun DI, Coskun Ü, Lemker T, Koch MHJ, Schägger H, Müller V (2001) Biochemistry 40:1890–1896
Guinier A (1939) Ann Phys (Paris) 12:161–237
Gibbons C, Montgomery MG, Leslie AG, Walker JE (2000) Nat Struct Biol 7:1055–1061
Ide T, Bäumer S, Deppenmeier U (1999) J Bacteriol 181:4076–4080
Inatomi K-I, Eya S, Maeda M, Futai M (1989) J Biol Chem 264:10954–10959
Konarev PV, Volkov VV, Sokolova AV, Koch MHJ, and Svergun DI (2003) J Appl Crystallogr 36:1277–1282
Laemmli, UK (1970) Nature 227:680–685
Lemker T, Grüber G, Schmid R, Müller V (2003) FEBS Lett 544:206–209
Lingl A, Huber H, Stetter KO, Mayer F, Kellermann J, Müller V (2003) Extremophiles 7:249–257
Maegawa Y, Morita H, Yao M, Watanabe N, Tanaka I (2004) Acta Cryst D60:1484–1486
Makyio H, Iino R, Ikeda C, Imamura H, Tamakoshi M, Iwata M, Stock D, Bernal RA, Carpenter EP, Yoshida M, Yokoyama K, Iwata S (2005) EMBO J 24:3974–3983
Müller V, Grüber G (2003) Cell Mol Life Sci 60:474–494
Olendzenski L, Hilario E, Gogarten JP (1998) In: Horizontal Gene Transfer, Syvanen K, Kado CI (eds), Chapman & Hall, New York, pp 349–362
Pedersen PL, Ko YH, Hong S (2000) J Bioenerg Biomembr 32:325–332
Provencher SW (1982) Comput Phys Commun 27:213–227
Radermacher M, Ruiz T, Wieczorek H, Grüber G (2001) J Struct Biol 135:26–37
Roos M, Soskic V, Poznanovic S, Godovac-Zimmermann J (1998) J Biol Chem 273:924–931
Schäfer G, Engelhard M, Müller V (1999) Mol Biol Rev 63:570–620
Schäfer I, Bailer SM, Düser MG, Börsch M, Bernal RA, Stock D, Grüber G (2006) J Mol Biol 358:725–740
Screerama N, Woody RW (1993) Anal Biochem 209:32–44
Senior AE, Nadanaciva S, Weber J (2000) J Exp Biol 203:35–40
Stan-Lotter H, Hochstein LI (1989) Eur J Biochem 179:155–160
Svergun DI (1992) J Appl Crystallogr 25:495–503
Svergun DI (1993) J Appl Crystallogr 26:258–267
Svergun DI (1997) J Appl Crystallogr 30:792–797
Svergun DI, Konrad S, Huß M, Koch MHJ, Wieczorek H, Altendorf K, Volkov VV, Grüber G (1998) Biochemistry 37:17659–1766
Svergun DI, Bećirević A, Schrempf H, Koch MH J, Grüber G (2000) Biochemistry 39:10677–10683
Svergun DI, Petoukhov MV, Koch MHJ (2001) Biophys J 80:2946–2953
Svergun DI, Koch MHJ (2002) Curr Opin Struc Biol 12:654–660
Uhlin U, Cox GB, Guss JM (1997) Structure 5:1219–1230
Vaaje-Kolstad G, Houston DR, Riemen AHK, Eijsink V GH, van Aalten DMF (2005) J Biol Chem 280:11313–11319
Wilkins MR, Lindskog I, Gasteiger E, Bairoch A, Sanchez JC, Hochstrasser DF, Appel RD (1997) Electrophoresis 18:403–408
Wilkens S, Dahlquist FW, McIntosh LP, Donaldson LW, Capaldi RA (1995) Nature Struct Biol 2:961–967